and Figure (f) show the track p_t and p distributions. The signal and background all fall in the low energy range where it is difficult to separate electrons and pions.

5.3 Final selection based on event topology

The signature of diffractive $J/\psi \rightarrow e^+e^-$ is very clear: nothing but a pair of e^+e^- of invariant mass 3.1 GeV is detected in the main detector. However, the identification of an electron and an accurate measurement of its momentum vector are challenging tasks for a new detector. Measurement difficulties were exacerbated by a lack of forward and rear tracking chambers. Track momentum uncertainty is large if the track has a large dip angle and penetrates fewer superlayers of the CTD.

The final selection criteria of diffractive $J/\psi \rightarrow e^+e^-$ consisted of following requirements:

(1) Topological feature:

  a. only one pair of oppositely charged tracks with two clusters matched.

  b. energy in CAL not related to e^+e^- be less than 1 GeV.

(2) Kinematic region: $40\text{GeV} < \sqrt{s_{\gamma p}} < 140\text{GeV}$

(3) Accuracy in momentum measurement: track rapidity $|\eta| < 1.5$

(4) Track $p_t > 0.5$GeV (to reject pions).

(5) Electron identification.

Not all of these cuts can be applied with same confidence. For example, requirement(5) is a big challenge. The ZEUS calorimeter was designed for detection of the ep scatterings at very short distances(very hard scatterings). Separation of low energy(about 1.5 GeV) electrons and pions is not relevant to very hard scatterings. While low energy electrons can be well identified by dE/dx measurement along the tracks, it requires special efforts to reduce the 12% error in dE/dx measurement in the 1993 data. Therefore, requirement(5) is reserved only as a last resort. It is clear a two step event selection is advantageous.

In the first step, *diffractive events* were selected by applying criteria (1). Criteria (1.b) was also applied, requiring:

$$E_{\mathrm{CAL}} - E_{e^+} - E_{e^-} - DUEMC - DUHAC < 1\mathrm{GeV} \tag{50}$$

where $E_{e^+}(E_{e^-})$ is the energy deposited by $e^+(e^-)$ in the calorimeter, E_{CAL} is the total energy deposit in the calorimeter, $DUEMC$ and $DUHAC$ are energy sums over *isolated* EMC cells with energy below 80 MeV and isolated HAC cells with energy below 140 MeV respectively. The procedure of excluding contributions from the low energy *isolated* calorimeter cells is known as the depleted uranium(DU) *noise suppression*. This is different from the *Zero suppression* which had been done by the online TLT and the offline reconstruction, when *any* EMC cells with energy below 60 MeV and *any* HAC cells with energy below 110 MeV(or 100 MeV, depending on the cell location) were removed from the event data.

Among 13,612 events in the pre-selection sample, 1,155 events passed the *diffractive* test. In Figure 30(a), near 3.1 GeV, the J/ψ invariant mass peak stands above the background. Only 91 events fall in the region 2.85GeV $< Mass <$ 3.25GeV, very close to that of the final selection(76 events). Figure 30(b) shows $\sqrt{\gamma p}$ distribution of the diffractive events with shaded part corresponding to events under the J/ψ mass peak.

As a check of the performance of the triggers during the 1993 runs, the number of diffractive events accepted by a specified trigger is plotted against the integrated luminosity (Figure 30(c) and (d)). For a stable trigger, this curve should be a straight line of a constant slope within fluctuations. The slope of TLT l^+l^- trigger changed from 1.1nb to 1.6nb after its modification in the middle of the 1993 runs. This increase was due to an enhanced efficiency in track-cluster matching in the forward direction.

The cuts in the second step of the final selection are to some extent arbitrary, in that minor modification of these cuts would not dramatically affect the result. With the small diffractive sample of 1,155 events, it is easy to test and compare

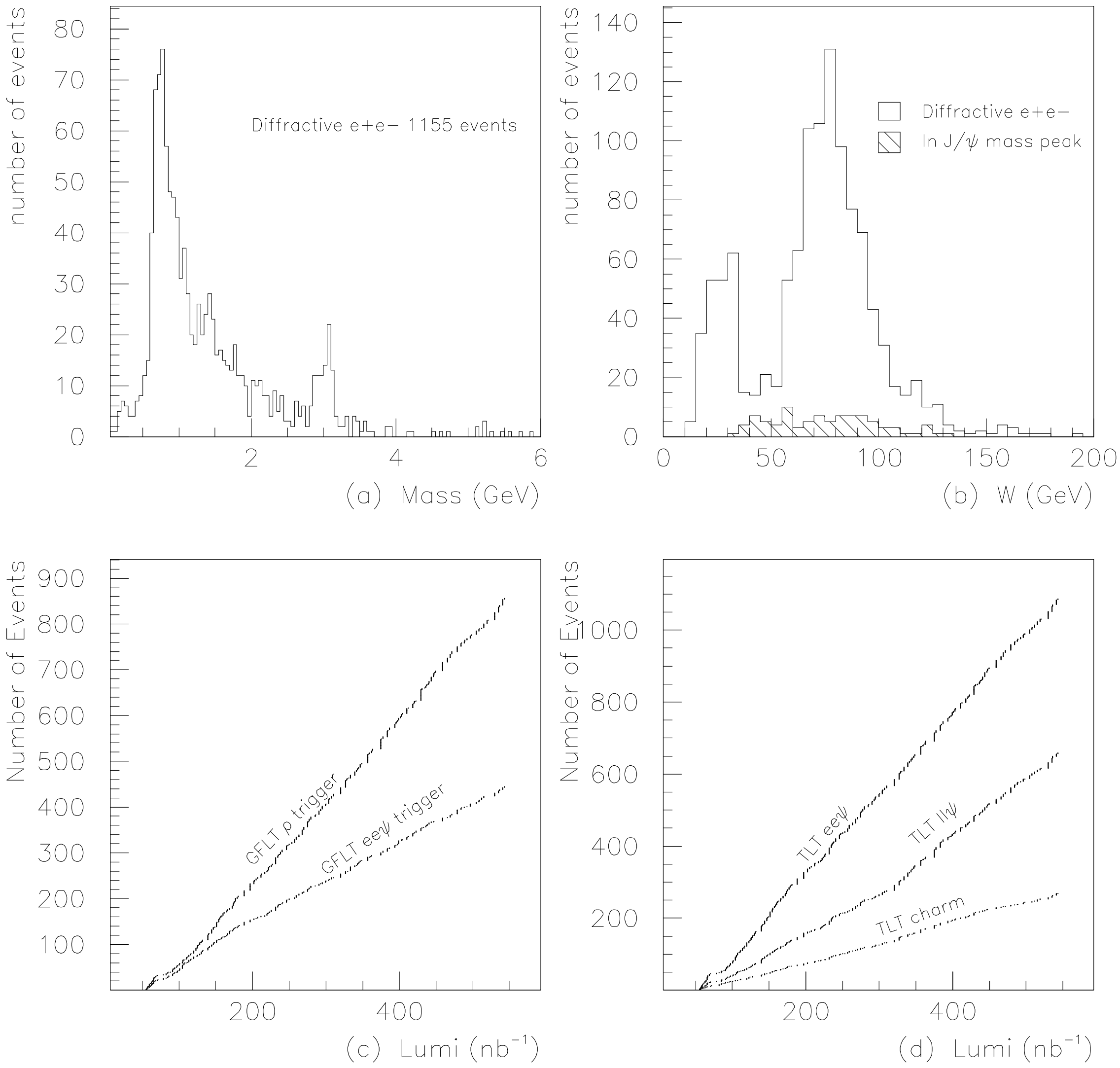

Figure 30: Profile of the diffractive sample. (a) The invariant mass histogram. The J/ψ peak is clearly observed near 3.1 GeV. (b) $\sqrt{s_{\gamma p}}$ histogram. Shaded part corresponds to events under the J/ψ mass peak. (c) and (d) Number of events accepted by each contributing GFLT and TLT triggers versus the integrated luminosity. The slope of TLT l^+l^- changed from 1.1nb^{-1} to 1.6nb^{-1} at the integrated luminosity$=$ 310nb^{-1}, when this filter was modified.

various variations of the final selection criteria. The goal of candidate selection is to obtain a sample of high purity, well determined acceptance and high statistics. $\rho\sqrt{n}$(see Eq. (49)) is about the same using different cuts. Uncertainty in acceptance ($\Delta\epsilon/\epsilon$) is a major concern. Therefore, we choose to apply simple cuts on the kinematics variables, and very conservative cuts on calorimeter responses.

Table 16: Final selection of $J/\psi \rightarrow e^+e^-$ candidates

selection criteria	remaining events	mass=2.85-3.25 GeV
pre-selection	13,612	1,450
diffractive	1,155	91
$40 < \sqrt{s_{\gamma p}} < 140$	904	86
$-1.5<$track rapidity<1.5	494	76
track $p_t > 0.5$ GeV	284	76
EMC > 99% Etotal	268	73
track-cluster matching quality	210	67

Final selection criteria and effects are shown in Table 16. Effects of $\sqrt{s_{\gamma p}}$, track rapidity η, p_t and the invariant mass cuts on the diffractive sample are also shown in Figure 31. Most background in the low mass and low $\sqrt{s_{\gamma p}}$ regions were removed by these kinematic cuts which have little effect on events in the J/ψ mass peak region. Most of the background events in the J/ψ mass peak region were removed by the diffractive cuts. This indicates that the background and signals are well separated in the kinematic phase space. In contrast, inelastic $J/\psi \rightarrow e^+e^-$ events and background are not well separated in the phase space and therefore the extraction of inelastic $J/\psi \rightarrow e^+e^-$ signals relies much on the detector's ability in electron hadron separation.

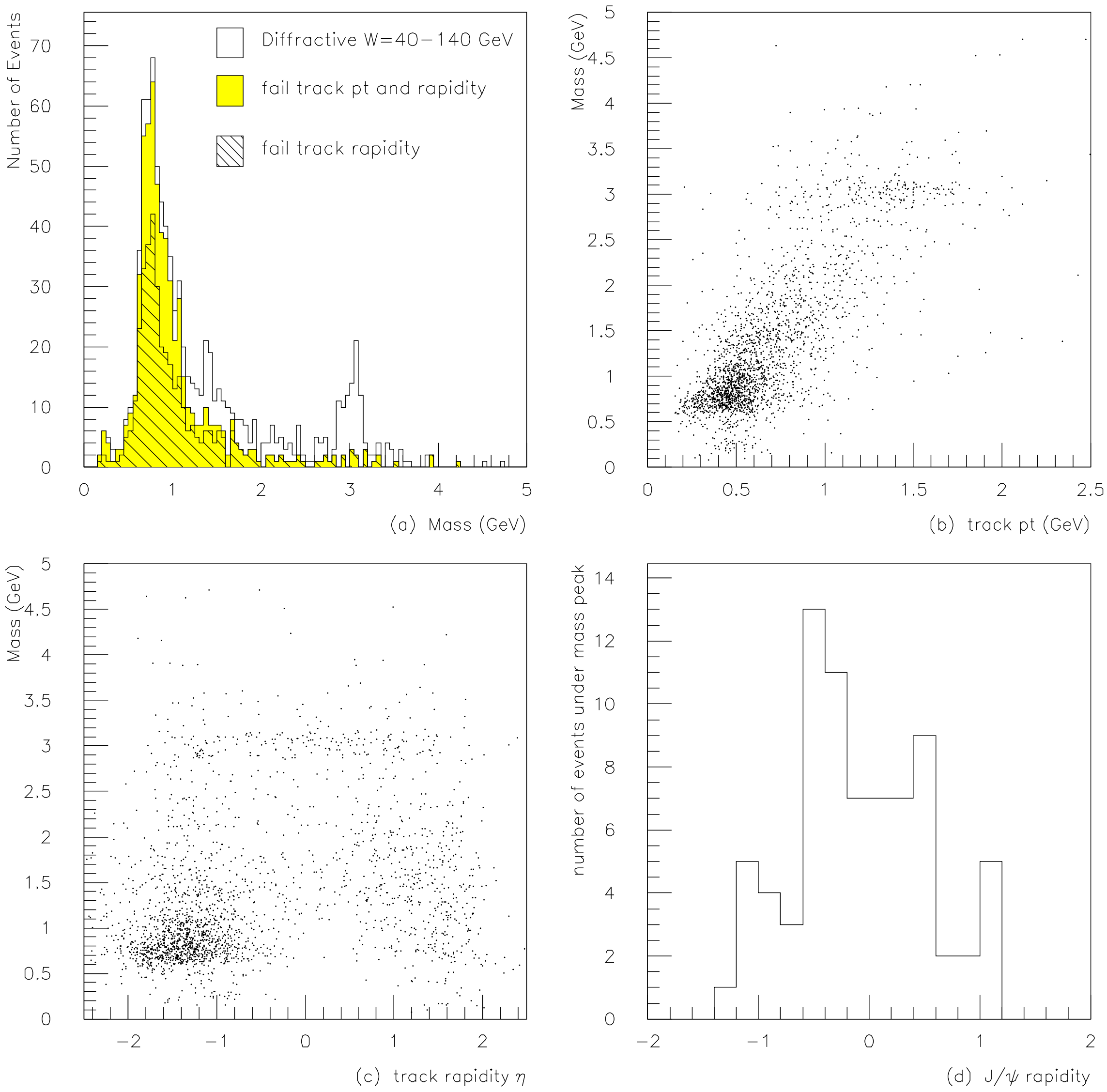

Figure 31: Profile of the final selection. (a) Invariant mass distribution of the diffractive sample after a cut on $\sqrt{s_{\gamma p}}$. The shaded area marks the number of events removed by cuts on track rapidity $|\eta|$ and track p_t. (b) Scatter plot of mass versus track p_t of the diffractive sample (c) Scatter plot of mass versus track rapidity η of the diffractive sample (d) Rapidity distribution of the 76 candidates.